

Flexural behavior and impact resistance of high-strength concrete containing micro-steel and macro-polyolefin fibers

Oveys Afzali-Naniz^a, Arash Ashouri-Seynaki^b and Moosa Mazloom^{*}

Department of Structural and Earthquake Engineering, Faculty of Civil Engineering, Shahid Rajaei Teacher Training University, I. R. Iran

(Received November 17, 2024, Revised March 21, 2025, Accepted April 12, 2025)

Abstract. This paper investigates the effects of micro-steel fibers (MSF) and macro-polyolefin fibers (MPF) on the flexural behavior and impact resistance of high-strength concrete (HSC). For this purpose, eleven mix compositions with four different volume fractions of MPF (0.25%, 0.5%, 75% and 1%), four volume fractions of MSF (0.25%, 0.5%, 75% and 1%), and also three mixes with the combination of micro-steel and macro-polyolefin fibers at a total fiber volume fraction of 1.0% were designed. The compressive strength, post-crack behavior, flexural behavior, and impact resistance were studied. The highest equivalent flexural strength ratios were achieved in hybrid mixes combining MSF and MPF, reaching up to 79.1% for the M25-75 mix, indicating the synergistic benefits of fiber hybridization. Moreover, the flexural performance test indicated that the energy absorption capacity was significantly larger for the hybrid mixes. The results showed that while MPF mixes exhibited higher impact resistance at the first crack for a given fiber volume fraction, the hybrid fiber mixes displayed the best overall impact resistance at failure.

Keywords: flexural behavior; high strength concrete; impact resistance; macro-polyolefin fibers; micro-steel fiber

1. Introduction

Normal strength concrete has significant limitations in terms of achieving today's performance and durability standards (Xue *et al.* 2020, Mazloom 2023). Modern advancements in civil engineering construction have made a critical need for new types of concrete that should have better properties, including high-strength, toughness, and durability. (Farnam *et al.* 2010, Breitenbuecher 1999). The use of high-strength concrete (HSC) has become increasingly popular in recent years due to its exceptional compressive strength and durability properties (Shen *et al.* 2019, Shen *et al.* 2020). However, high-strength concrete exhibits some disadvantages, such as its brittle behavior and susceptibility to cracking. This can lead to a reduction in the flexural behavior and long-term durability of structures.

Many studies have proposed the use of different types of fiber in HSC. Actually, the addition of

^{*}Corresponding author, Professor, E-mail: mazloom@sru.ac.ir

^aResearch Assistant, E-mail: oveys.afzali@sru.ac.ir

^bM.Sc., E-mail: toashouri@gmail.com

fibers helps overcome the low tensile strength of concrete. Furthermore, when concrete cracks, it becomes more ductile since the presence of multiple cracks prevents the effective transfer of tensile stresses. Obviously, the dosage, type, and shape of the fibers have a significant impact on how concrete behaves (Ganesan and Shivananda 2000, Fallah and Nematzadeh 2017). Today, the most commonly used fibers are steel, glass, carbon, and synthetic (mostly polypropylene) fibers. Fibers can be categorized into two groups of macro-synthetic and micro-synthetic. Micro-synthetic fibers have a diameter up to 0.3mm, while macro-synthetic fibers have a diameter greater than 0.3mm (ACI 544.3R 2008). The plastics industry facilitates the development of a novel generation of synthetic fibers. These fibers exhibit no chemical reactivity when exposed to alkaline conditions, making them suitable for use in concrete. The manufacturing process entails converting a homopolymeric resin into a monofilament form, resulting in the production of polyolefin fibers (Alberti *et al.* 2019, Alberti *et al.* 2020). Among various types of fibers, steel fibers are the most widely utilized in concrete reinforcement (Sorelli *et al.* 2006, Cuenca, *et al.* 2015). Additionally, over the past decade, macro-synthetic fibers have undergone substantial improvements, enabling them to impart significant toughness and durability to concrete matrix (Navas *et al.* 2018, Conforti *et al.* 2017).

Altalabani *et al.* (2020) stated that incorporating macro-polypropylene fibers or a combination of micro and macro-polypropylene fibers into self-compacting lightweight concrete significantly enhanced impact and flexural performance when compared to using micro fibers alone. Self-compacting concrete (SCC) is famous for its exceptional flowability and resistance to aggregate segregation (Mazloom *et al.* 2020, Mazloom *et al.* 2019, Mazloom *et al.* 2015, Nikzad *et al.* 2024, Mazloom and Charmsazi 2024). In research conducted by Hadeed *et al.* (2023), a combination of glass fibers and polypropylene fibers was used in the production of HSC and lightweight concrete (LWC) mixes. Their findings revealed that incorporating 0.7% glass fibers led to the greatest improvements in compressive strength, tensile splitting strength, and flexural strength for both the HSC and LWC mixtures. Moreover, when assessing the performance through compressive strength tests, tensile splitting tests, and flexural strength tests, the glass fibers exhibited better results and led to greater improvements in strength properties compared to the polypropylene fibers.

Song and Wang (2004) investigated the effects of incorporating steel fibers into high-strength concrete mixtures. They varied the steel fiber dosage from 0.5% to 2.0% by volume fraction. Their results showed that when 1.5% steel fibers were added, there was a 15.3% increase in the compressive strength of the concrete. At the highest dosage of 2.0% steel fiber volume fraction, they observed improvements in both the splitting tensile strength and the flexural strength of the fiber-reinforced high-strength concrete compared to the plain concrete without fibers. Antarvedi *et al.* (2023) investigated the effects of two different types of steel fibers (crimped steel fibers and hooked-end steel fibers) into concrete mixes, using each type of steel fiber separately in combination with polypropylene fibers. Their findings revealed that the inclusion of steel fibers was more efficacious in enhancing the flexural strength characteristics of the concrete and impeding the propagation of cracks, compared to when only polypropylene fibers were used.

Fracture energy is the energy required to propagate a crack per unit area of the crack surface (Ahmadi *et al.* 2024a, Ahmadi *et al.* 2024b, Mazloom and Mirzamohammadi 2021, Mazloom *et al.* 2021). Mazloom *et al.* (2023) studied the effects of macro-polyolefin fibers on the fracture energy of high strength concrete. Their result indicated that the fracture energy of high-strength concrete highly depended on the dosage of macro-fibers. Karamloo *et al.* (2020) investigated the effects of different amount of macro-polyolefin fibers on the size effect and fracture behavior of self-

compacting lightweight concrete. In a study by Doostmohamadi *et al.* (2020), they assessed how the inclusion of macro- polyolefin fibers influences the bonding between glass fiber-reinforced polymer bars (GFRP) and self-compacting lightweight concrete. Their findings indicated that these fibers have the capability to restrict the formation of longitudinal cracks running parallel to the GFRP bars.

Polypropylene fibers are widely used in different kinds of cementitious composites (Karimpour and Mazloom 2023, Karimpour and Mazloom 2022). The study by Karimipour *et al.* (2021) looked at how silica fume and polypropylene fibers affected the properties of HSC in both hardened and fresh states. Their findings showed that increasing the amounts of nano-silica and silica fume powder resulted in reduced workability. Furthermore, silica fume had a more pronounced negative effect on workability compared to nano-silica. On the other hand, incorporating silica fume and polypropylene fibers led to increases in both compressive and tensile strengths of HSC. Hakeem *et al.* (2022) investigated how adding micro-steel fibers influenced both the workability and strength characteristics of ultra-high-performance concrete (UHPC) mixes that also contained nano-silica particles. Their study found that while the compressive strength of the UHPC was not significantly impacted by the inclusion of the micro-steel fibers, several other key mechanical properties were enhanced. Specifically, they reported that the modulus of elasticity, flexural strength, and tensile strength of the UHPC were improved by incorporating the micro-steel fibers into the mix design.

While previous studies have examined how various fiber types influence concrete (Abna and Mazloom 2022, Mazloom *et al.* 2023, Mazloom *et al.* 2024, Mirzamohammadi and Mazloom 2021), there appears to be limited research on the flexural behavior and impact resistance of HSC containing micro-steel fibers (MSF) and macro-polyolefin fibers (MPF). This research focuses on MSF and MPF, exploring their effects on the flexural behavior and impact resistance of HSC. The objective of this study is to provide a comprehensive evaluation and comparison of the mechanical behavior of HSC reinforced with different types and dosages of fibers.

2. Experimental program

2.1 Material properties

In this research, type-II ordinary Portland cement was used. Furthermore, silica fume was utilized as a cement replacement material. Table 1 displays the chemical and physical properties of these materials. Crushed gravel with a maximum nominal size of 12mm and river sand with a fineness modulus around 3 were used as coarse and fine aggregates, respectively. To achieve the desirable workability, a kind of superplasticizer based on polycarboxylate was utilized. In addition, micro-steel fibers with high carbon alloy and macro-polyolefin fibers were utilized. The used fibers are shown in Fig. 1 and the properties of fibers are shown in Table 2.

2.2 Mix proportions and mixing procedure

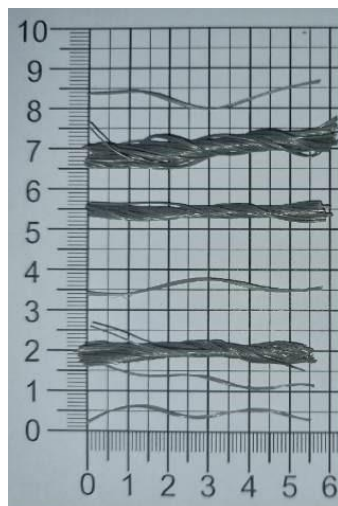
In this research, the effects of MSF and MPF on the flexural behavior and impact resistance of high-strength concrete were investigated. To achieve this, eleven mix compositions were designed, each with varying volume fractions of MPF (0.25%, 0.5%, 0.75%, and 1%), MSF (0.25%, 0.5%, 0.75%, and 1%), and a combination of both MPF and MSF at a total fiber volume fraction of 1.0%. Table 3 displays the mix proportions of the specimens.

Table 1 Chemical and Physical properties of the used cement and silica fume

Chemical analysis (%)	Cement	Silica fume
SiO ₂	20.4	95.1
CaO	62.3	0.6
Fe ₂ O ₃	3.7	0.4
Al ₂ O ₃	5.1	1.32
SO ₃	1.9	0.6
MgO	2.3	1
K ₂ O	0.7	1
Na ₂ O	0.4	-
L.O. I	1.7	-
Specific surface area (cm ² /g)	3300	200
Specific gravity (gr/cm ³)	3.15	2.5

Table 2 The properties of the used fibers

Properties	Shape	Length (mm)	Diameter (mm)	Aspect ratio	Tensile strength (MPa)	Elastic modulus (GPa)	Density (g/cm ³)
Macro-Polyolefin fibers	Twist	54	0.4	135	550	5	0.91
Micro-Steel fibers	Straight	16	0.25	64	2720	210	7.8



(a) Macro-polyolefin fibers



(b) Micro-Steel fibers

Fig. 1 Shape of the used fibers

The mixing procedure for all the mix designs followed the same protocol. The mixing process involved several steps as follows. To produce high-strength fiber-reinforced concrete, first, the aggregate materials, including sand and gravel, were mixed in a mixer for one minute. Then, the

Table 3 Mix proportions

Mix ID	Cement	Silica fume	Water	Fine Aggregate	Coarse Aggregate	MSF		MPF		SP
						Volume Fraction	weight	Volume Fraction	Weight	
						%	kg/m^3	%	kg/m^3	
MIX0	460	50	163	902	836	0	0	0	0	0.9
M00-25	460	50	163	899	833	0	0	0.25	2.28	1
M25-00	460	50	163	899	833	0.25	19.6	0	0	1
M00-50	460	50	163	895	830	0	0	0.5	7.55	1.2
M50-00	460	50	163	895	830	0.5	39.3	0	0	1.2
M00-75	460	50	163	892	827	0	0	0.75	6.83	1.25
M75-00	460	50	163	892	827	0.75	58.9	0	0	1.25
M00-100	460	50	163	889	823	0	0	1	9.1	1.35
M100-00	460	50	163	889	823	1	78.5	0	0	1.35
M25-75	460	50	163	889	823	0.25	19.6	0.75	6.83	1.35
M50-50	460	50	163	889	823	0.5	39.3	0.5	4.55	1.35
M75-25	460	50	163	889	823	0.75	58.9	0.25	2.28	1.35

fibers were added to the aggregate materials, and mixing continued at high speed until the fibers were fully mixed. In the hybrid mixes, first, MSF were added, and after one minute, MPF were added. Then, cement was gradually added to the mixer, and in the final step, a solution of water, superplasticizer, and silica fume that had been previously prepared was gradually poured into the mixer over a period of 30 seconds. The final mixture was mixed in the mixer for two minutes.

2.3 Testing methods

The slump and fresh unit weight tests were performed in accordance with ASTM C143 and ASTM C138, respectively (ASTM C 143 2020, ASTM C 138 2014). The mechanical properties of hardened concrete were tested using the following methods. The 28-day compressive strength of each mixture was obtained using three 150 mm cube specimens in accordance with BS1881: Part 116 (BS 1881, 1983). The flexural behavior test of fiber-reinforced concrete beams was conducted through a three-point bending test in accordance with the ASTM C 1609C/C1609M standard (ASTM C 1609 2012). This test aimed to record the flexural behavior (Fig. 2) and obtain the flexural modulus under various conditions, including maximum load, first crack, ultimate load, and energy absorption after the appearance of the first crack until final failure. Three identical specimens of each mix design were tested. The average result was recorded as the final outcome.

According to ACI 544.9R.17 (2017) the following parameters are determined to describe the flexural properties of high strength fiber reinforced concrete using Eqs. (1) and (2):

- a) Residual load values (P_{600}^D, P_{150}^D) at $\delta = L/600$ and $L/150$ of the span length L , (N).

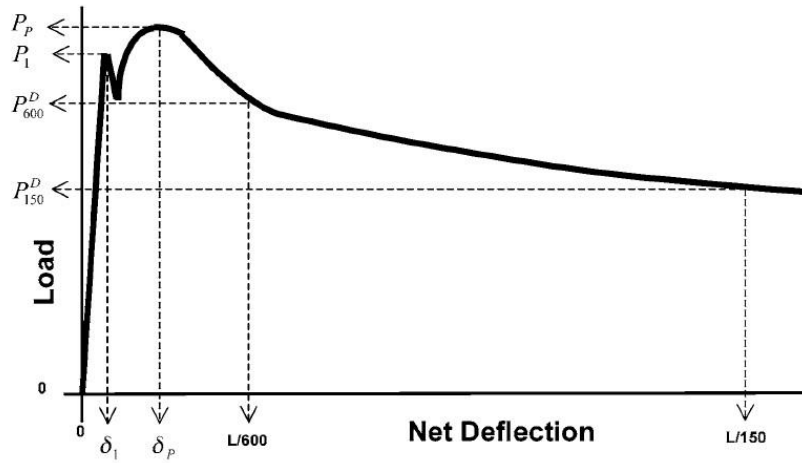


Fig. 2 Schematic load-deflection curve and related parameters (ASTM C1609 2012)

- b) Residual strength values (f_{600}^D , f_{150}^D) using P_{600}^D and P_{150}^D in Eq1, (MPa).
- c) T_{150}^D toughness, area under the P- δ curve up to $\delta = L/150$ of the span length L, (J).
- d) Equivalent flexural strength ratio (%) using Eq. (2).

$$f_1 = \frac{p \cdot l}{bd^2} \quad (1)$$

$$R_{T,150}^D = \frac{150T_{150}^D}{f_1 bd^2} \times 100 \quad (2)$$

where l is span length (mm), b is width (mm), d is depth (mm), P_l is first peak load (N), P_p is peak load (N), δ_l is net deflection at first peak load (mm), δ_p is net deflection at peak load (mm), f_l is first peak strength (MPa) and f_p is peak strength (MPa).

Repeated Blows Drop-Weight Impact (RBDWI) test method was used to evaluate the impact resistance. The RBDWI test is known as the easiest method to measure the impact resistance of fiber reinforced concrete. This test was conducted on six disc-shaped specimens for each mix design, with 155 mm diameter and 64 mm thickness, following the recommendations outlined in Section 9.2.1 of ACI544.9R-17 (2017). The average results from the six identical specimens of each mix design were recorded as the final outcome. In this test, as shown in Fig. 3, a disk specimen was placed inside a metal quadrangular frame on the bottom surface, and the space between the frame and the specimen was filled with elastic foam to prevent the specimen movement during the test. Then, a steel ball with a diameter of 57 mm was placed on the specimen. Multiple blows were inflicted on the steel ball by free fall of a 5.5 kg weight from a height of 550 mm. The number of blows until the appearance of the first visible crack was recorded for each specimen (N_1). After the creation of the first crack, the elastic foams between the frame and the specimen were removed, and according to the previous process, multiple blows were continued until the sample was destroyed. The number of blows required to destroy the sample was recorded as N_2 for each sample. Then the impact energy at the first crack (W1) and the impact energy (W2)

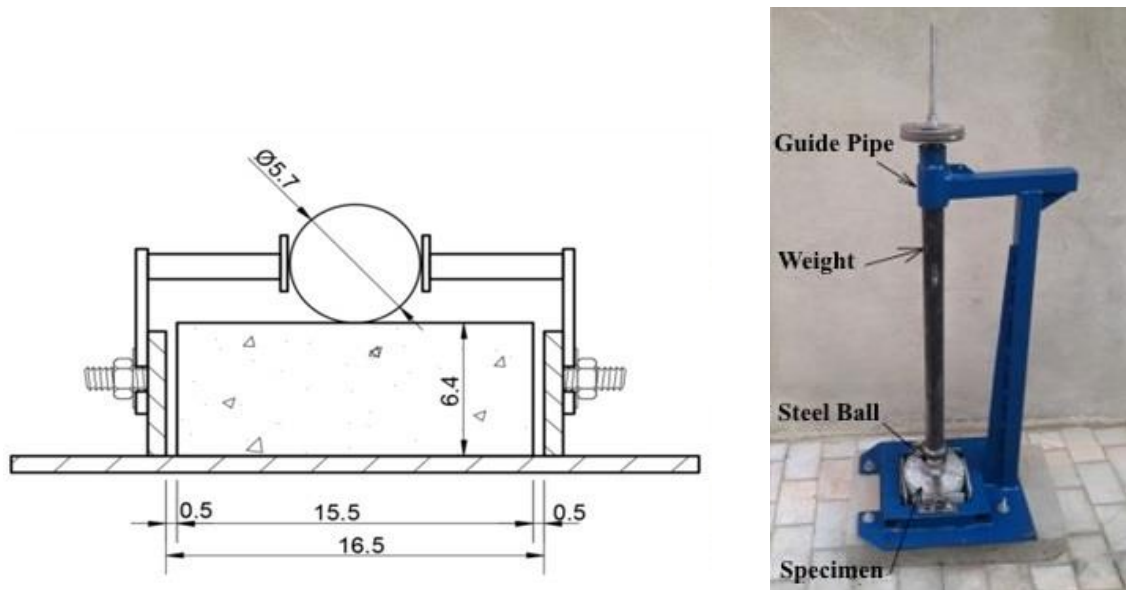


Fig. 3 Set up configuration of impact resistance test

at failure were obtained from Eq. (3) and Eq. (4). Also, the ductility index (β), which represents the resistance of concrete against deformation caused by impact after the first crack (or initial failure), was obtained from Eq. (5).

$$W_1 = N_1 \cdot mg \quad (3)$$

$$W_2 = N_2 \cdot mgh \quad (4)$$

$$\beta = \frac{(N_2 - N_1)}{N_1} \quad (5)$$

where N_1 is number of blows at first crack, N_2 is number of blows at failure, m is the mass of steel ball, h is drop-height, and g is the gravity acceleration.

3. Results and discussion

3.1 Fresh state properties

The slump and fresh unit weight results of HSC mixes are shown in Table 4. The results indicate that to achieve the same workability, the amount of superplasticizer consumed for the concrete samples containing fibers is higher than the control samples. Also, it can be inferred that as the fiber volume ratio and superplasticizer content increased, the slump loss remained relatively constant. This indicates that an increase in the fiber volume ratio reduced the workability. This decrease in workability was due to the lateral surface area of the fibers absorbing a greater amount of the cement paste, leading to a lower measured slump value (Guo *et al.* 2019).

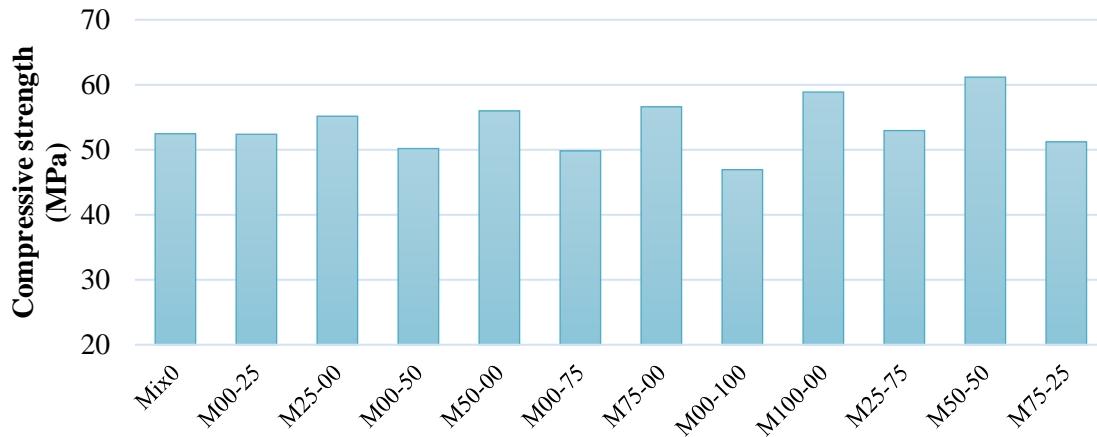


Fig. 4 Compressive strength of HSC with different percentages of MSF and MPF

Table 4 The slump and fresh unit weight results

Mix ID	Slump <i>mm</i>	Fresh unit weight <i>kg/m³</i>	Superplasticizer %
MIX0	60	2401	0.9
M00-25	50	2410	1
M25-00	55	2430	1
M00-50	50	2400	1.2
M50-00	45	2445	1.2
M00-75	60	2400	1.25
M75-00	50	2460	1.25
M00-100	60	2399	1.35
M100-00	55	2472	1.35
M25-75	40	2424	1.35
M50-50	60	2440	1.35
M75-25	65	2459	1.35

3.2 Mechanical properties of hardened concrete

3.2.1 Compressive strength

Fig. 4 displays the 28-day compressive strength results of HSC. The results revealed that with increasing the percentage of MPF, the compressive strength of concrete specimens slightly decreased. The highest decrease of compressive strength was in the mixes with 1% of MPF. Increasing the MPF by 1% reduced the compressive strength by 10.5%. On the other hand, with the increasing the percentage of MSF, the compressive strength of samples increased. Increasing MSF by volume fraction of 0.25%, 0.5%, 0.75% and 1% increased the compressive strength of HSC by 5.1%, 6.7%, 7.9% and 12.2%, respectively. The highest compressive strength was for

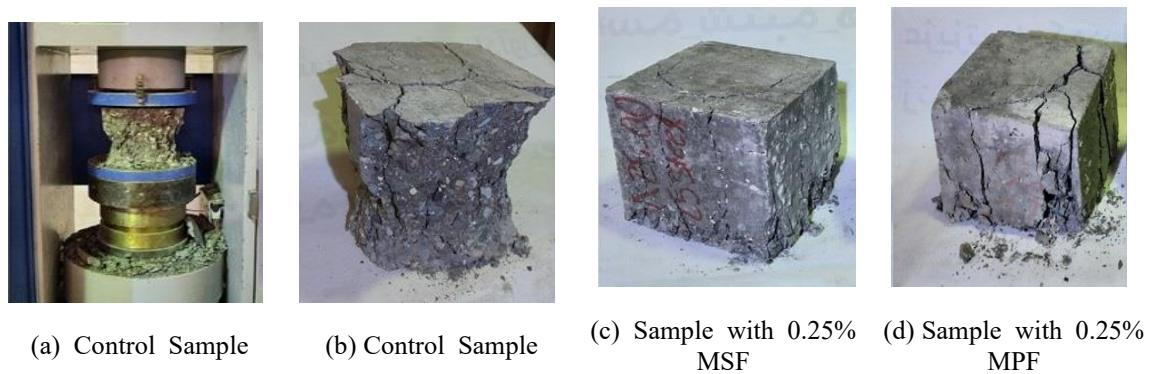


Fig. 5 Specimens after failure after compressive strength test

hybrid mixes with 0.5% MSF and 0.5% MPF, which increased by 16.5% compared to the control sample.

Although the compressive strength of M25-75 mixture is slightly higher than the control sample, and also the compressive strength of the M75-25 mixture is slightly less than the control sample, the difference between the compressive strength of these two mixtures and the control sample is insignificant. It can be concluded that the addition of MSF either individually or in combination with MPF in the volume fractions mentioned in this research causes a slight increase in compressive strength. Some studies have reported that the use of fibers in concrete has an increasing role in compressive strength, but it has also been found in some research that the addition of fibers in concrete has reduced the compressive strength. Alberti *et al.* (2020) reported that the effects of 3, 4.5, 6 and 10 kg/m³ of MPF on the compressive strength of normal concrete were insignificant. Hakeem *et al.* (2022) stated that the influence of micro-steel fibers on the compressive strength of the UHPC was not significant.

Fig. 5 shows some specimens after failure under the compressive strength tests. The samples without any fiber reinforcement exhibited a brittle failure mode, meaning they fractured in a sudden and abrupt manner. In contrast, failure of samples contained fiber was ductile. In samples with 0.25% MSF, the number of cracks were visually less than specimen with 0.25% MPF.

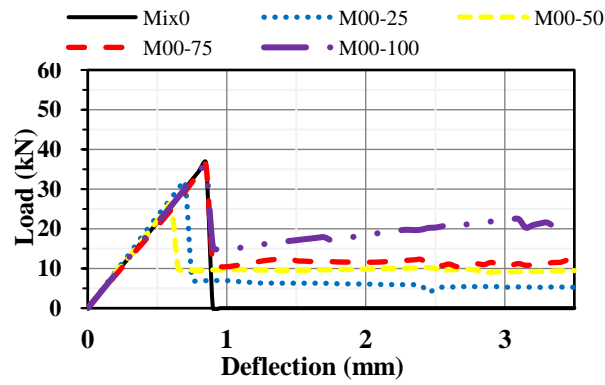
3.2.2 Flexural behavior

3.2.2.1 Load-deflection curve and related parameters

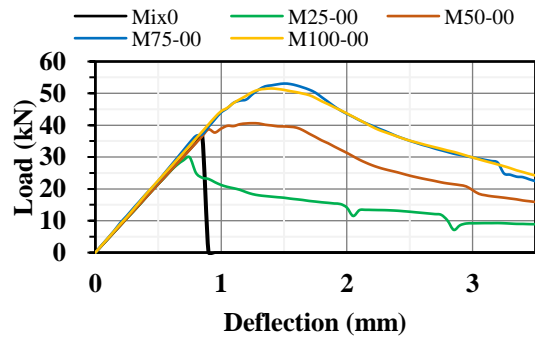
Fig. 6 displays the load deflection curves of HSC mixes reinforced with different volume fractions of MSF and MPF. Table 4 shows the flexural parameters based on ASTM C1609. As can be seen in Figs. 6 and 7, the failure of the control sample (Mix0) occurs abruptly and immediately after the formation of the first crack, exhibiting a clear brittle failure mode. However, the failure mechanism of mixes containing fibers was ductile (Fig. 7(b)). Typically, during these flexural behavior tests on simply supported beams, two distinct responses can be observed: (a) deflection-hardening or (b) deflection-softening. If the fiber-reinforced concrete can bear higher loads even after the initial cracking occurs, this phenomenon is referred to as deflection-hardening. On the other hand, if the load-bearing capacity decreases after the initial cracking, it is known as deflection-softening (Shi *et al.* 2020). It is apparent from Figs. 6(a)-6(c) that:

- After initial cracking, in HSC mixes reinforced with MPF, the load bearing capacity decreased (deflection-softening) but in HSC mixes with MSF or hybrid mixes, the load

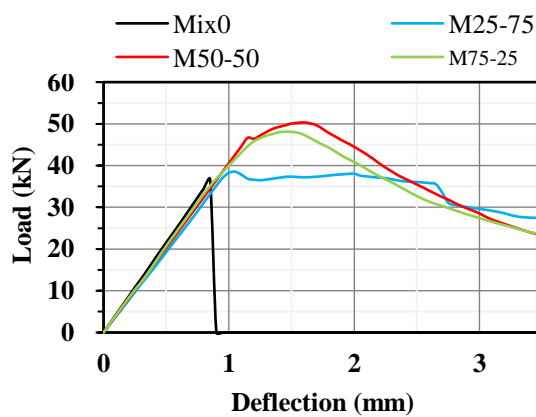
bearing increased (deflection-hardening). This different behavior could be due to the fact that MSF has a higher Young's modulus in compare with MPF.



(a) Mixes with MSF



(b) Mixes with MPF



(c) Hybrid mixes

Fig. 6 Load deflection curves of HSC mixes

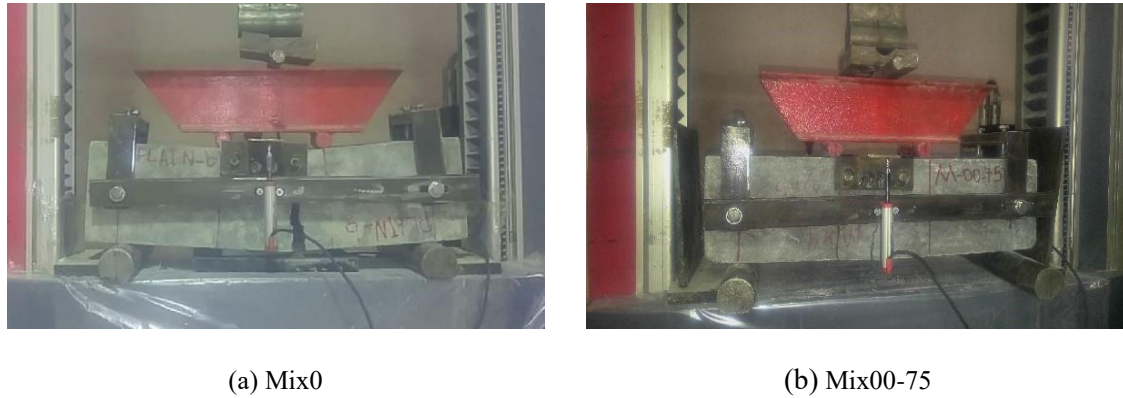


Fig. 7 Failure mechanism under flexural load

Table 5 The flexural parameters based on ASTM C1609

Mix ID	P_p	f_p	δ_p	P_{600}^D	f_{600}^D	P_{150}^D	f_{150}^D	T_{150}^D	$R_{T,150}^D$
	kN	MPa	mm	kN	MPa	kN	MPa	J	%
MIX0	36.7	4.9	0.86	32.4	4.3	0.0	0.0	16.1	14.6
M00-25	31.7	4.2	0.69	7.3	1.0	5.4	0.7	25.5	26.8
M25-00	30.0	4.0	0.75	29.9	4.0	9.2	1.2	47.3	52.6
M00-50	26.0	3.5	0.61	9.5	1.3	9.2	1.2	31.6	40.4
M50-00	42.9	5.7	1.32	31.8	4.2	19.6	2.6	83.8	72.7
M00-75	36.1	4.8	0.62	31.7	4.2	11.6	1.5	40.6	37.4
M75-00	53.1	7.1	1.5	34.5	4.6	29.9	4.0	99.5	74.9
M00-100	35.5	4.7	0.85	32.7	4.4	22.2	3.0	55.0	51.5
M100-00	53.6	7.2	1.42	33.5	4.5	29.9	4.0	107.2	69.8
M25-75	38.5	5.1	1.03	29.1	3.9	29.6	3.9	91.4	79.1
M50-50	50.3	6.7	1.57	30.4	4.1	28.5	3.8	104.1	74.4
M75-25	48.3	6.4	1.48	31.2	4.2	27.4	3.7	99.7	68.8

- The incorporation of MPF did not enhance the peak load capacity. In fact, the mixes containing 0.25% and 0.5% MPF exhibited a reduced peak load compared to the control sample without any fibers. However, in the case of hybrid mixes, which combined MPF with MSF, and mixes containing only MSF, the peak load exceeded that of the control sample.
- The area under the load-deflection curve, which represents the energy absorption capacity, was significantly larger for the hybrid mixes and the mixes containing only MSF when compared to the mixes reinforced solely with MPF.
- The volume fraction of fibers incorporated into HSC substantially impacts its load-deflection behavior. The quantity of fibers plays a pivotal role in determining the post-

peak load-carrying capacity of the concrete specimens. In other words, the dosage of fibers added to the concrete mix significantly influences its performance and load-bearing ability after reaching the maximum load.

3.2.2.2 Flexural strength

Fig. 5 presents the flexural strength results of high-strength concrete (HSC) mixes with different volume fractions of MSF and MPF. The results demonstrate that all mixes containing only MPF exhibited lower flexural strength than the control mix; however, at higher volume fractions, this difference was insignificant. On the other hand, mixes containing only MSF in volume fractions greater than 0.25% demonstrated the best performance in increasing flexural strength. In the mixtures containing only MSF at volume fractions of 0.50%, 0.75%, and 1.0%, respectively, an increase in flexural strength of 16%, 45%, and 47% was observed. Flexural strength also increased in hybrid mixes, though this increase was less than the similar mix design containing 0.1% MSF but higher than the similar mix design containing 0.1% MPF. Overall, the mix designs M100-00, M75-00, M50-50, and M75-25 exhibited the best performance in increasing the flexural strength, with increases of 47%, 45%, 37%, and 31%, respectively. Additionally, the mix designs M00-50 and M00-25 demonstrated the worst performance in reducing flexural strength, with reductions of 27% and 14%, respectively. Song and Hwang showed that the addition of steel fibers up to 0.2% by volume increases flexural strength; the amount of this increase depends on the volume fractions of the fibers and ranges from 28% to 127% (Song *et al.* 2004).

3.2.2.3 Flexural toughness

Flexural toughness characterizes the energy dissipation potential of fiber-reinforced composites under flexural loading conditions. It (T_{150}^D) refers to the total area under the load-deflection curve up to a net deflection of L/150 of the span length. The results of flexural toughness of HSC mixes with different volume fractions of MSF and MPF are shown in Table 5 and Fig. 9. As can be

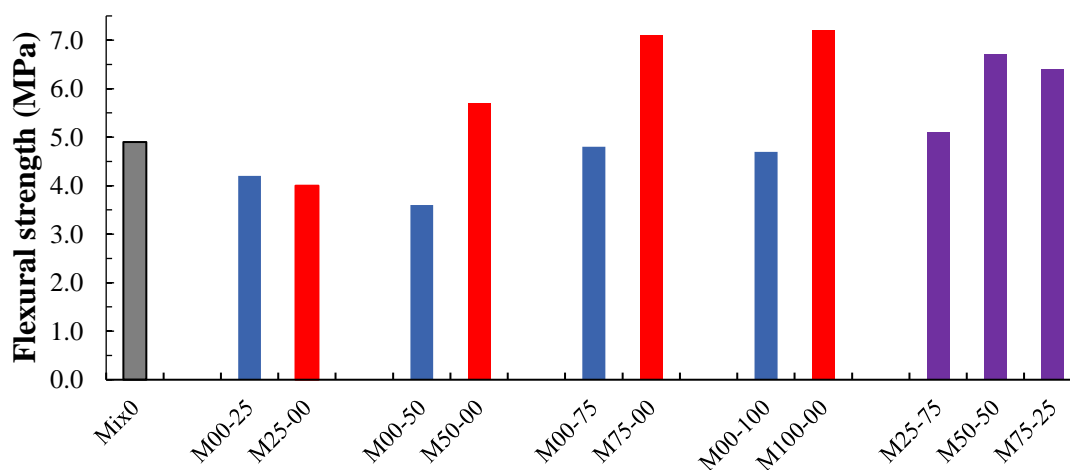


Fig. 8 Flexural strength of HSC mixes with different volume fractions of MSP and MPF

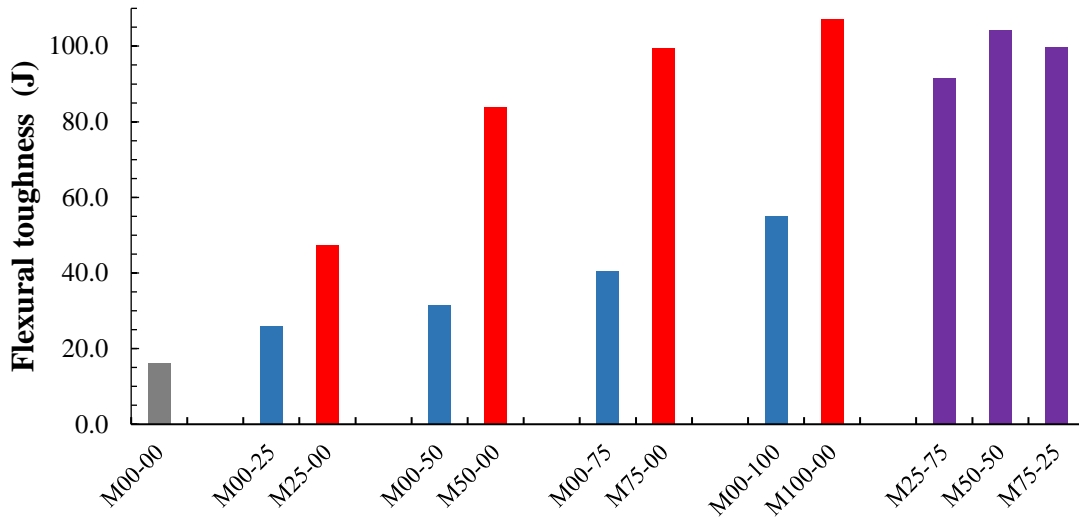


Fig. 9 Flexural toughness of HSC mixes with different volume fractions of MSP and MPF

seen, a significant growth in T_{150}^D was observed by increasing the volume fractions of fibers. The flexural toughness of mixes containing only MSF in volume fractions of 0.25%, 0.50%, 0.75% and 1.0% were 2.93, 5.2, 6.18 and 6.65 times that of the control sample, respectively. Whereas, the flexural toughness in mixes containing only MPF in the same volume fractions of 0.25%, 0.50%, 0.75% and 1.0% were about 1.6, 1.96, 2.51 and 3.41 times that of the control sample, respectively. Mixes containing hybrid fibers also showed good performance in terms of improving flexural toughness. The flexural toughness in three hybrid mixes of M75-25, M50-50 and M25-75 were 5.67, 6.46 and 6.2 times that of the control mix, respectively.

3.2.2.4 Equivalent flexural strength ratio

Equivalent flexural strength ratio ($R_{T,150}^D$) primarily depends on the first peak strength and flexural toughness. In calculating the equivalent flexural strength ratio by dividing the toughness by first peak strength, it is possible to eliminate the effect of this strength on the reduction or increase of energy absorption. The results of the equivalent flexural strength ratio of HSC mixes with different volume fractions of MSF and MPF are shown in Table 5 and Fig. 10. As can be seen, the equivalent flexural strength ratio of HSC mixes containing MSF was higher than that of mixes containing MPF at the same volume fractions. The equivalent flexural strength ratios of mixes containing only MSF in volume fractions of 0.25%, 0.50%, 0.75%, and 1.0% were 52.6%, 72.2%, 74.9%, and 69.8%, respectively. Whereas, the equivalent flexural strength ratios of mixes containing only MPF in the same volume fractions of 0.25%, 0.50%, 0.75%, and 1.0% were about 26.8%, 40.4%, 37.4%, and 51.7%, respectively. The hybrid mixes of MSF and MPF led to better equivalent flexural strength ratios. For the three hybrid mixes of M25-75, M50-50, and M75-25, the equivalent flexural strength ratios were 79.1%, 74.4%, and 68.8%, respectively.

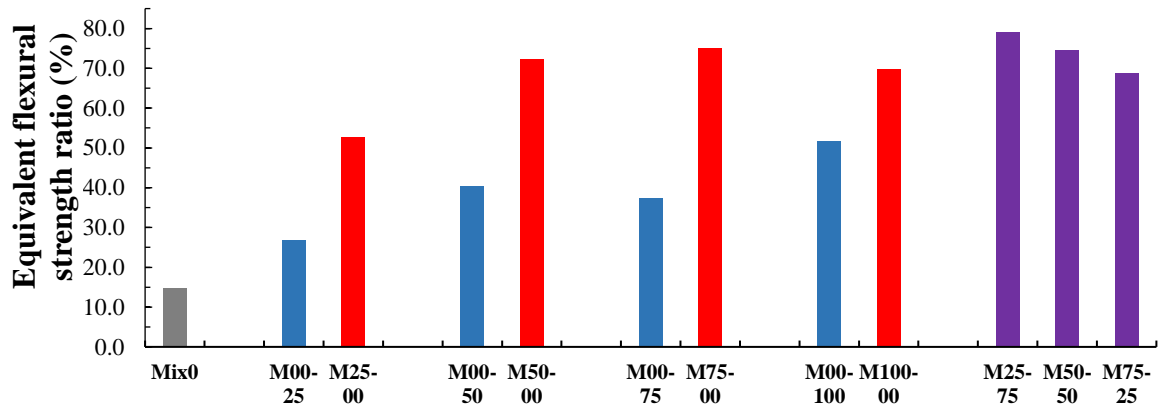


Fig. 10 Equivalent Flexural strength ratio of HSC mixes with different volume fractions of MSP and MPF

Table 6 The results of RBDWI test

Mix ID	N_1	N_2	Average		W_1	W_2	β
			N_1	N_2	J	J	%
MIX0	3·3· 2· 3·2· 4	6· 4· 4· 5· 4· 8	3	5	90.8	151.3	0.7
M00-25	7· 7· 2·3· 25	24· 75· 42· 75· 71	9	57	272.3	1724.3	5.3
M25-00	3·14·3· 4·5·3	20· 35· 24· 30· 28· 23	9	27	151.3	816.8	4.4
M00-50	27· 13· 48· 6· 64· 19	150· 149· 203 ·134 ·124 ·93	30	142	907.5	4295.5	3.7
M50-00	12·6·5·7· 8· 7	41· 57· 42· 35· 34· 38	8	41	242.0	1240.3	4.1
M00-75	23· 10· 72· 61· 56	152· 309· 226· 273· 189	44	230	1331.0	6957.5	2.3
M75-00	91· 24· 21· 29· 15· 28	242· 166· 192· 256· 123· 139	35	186	1058.8	5626.5	4.3
M00-100	16· 5· 26· 31· 23· 36	105· 137· 115· 245· 163· 213	23	163	695.8	4930.8	6.1
M100-00	15· 32· 21· 17· 27· 9	211· 239· 93· 117· 146· 53	20	143	605.0	4325.8	6.2
M25-75	18· 9· 10· 17· 13	243· 260· 286· 296· 209	13	259	393.3	7834.8	18.9
M50-50	13· 33· 29· 22· 37· 28	276· 177· 385· 340· 407· 433	27	336	816.8	10164.0	11.4
M75-25	18· 8· 9· 12· 15· 34	171· 80· 188· 183· 161· 157	16	157	484.0	4749.3	8.8

3.2.3 Impact resistance

The results of impact resistance based on RBDWI test method are shown in Table 6 and Fig. 11.

The impact resistance of all mixes containing fiber were much better than the control sample. The impact energy at the first crack (W_1) for HSC Specimens with 0, 0.25%, 0.5%, 0.75% and 1% MSF were 90.8, 151.3, 242, 1058.8 and 605 J, respectively, while their corresponding values at failure (W_2) were 151.3, 816.3, 1240, 5626.5 and 4325.8J, respectively. The impact energy at the first crack (W_1) for HSC Specimens with 0, 0.25%, 0.5%, 0.75% and 1% MPF were 90.8, 272.3, 907.5, 1331, and 695J respectively, while the impact energy at failure (W_2) were 151.3,

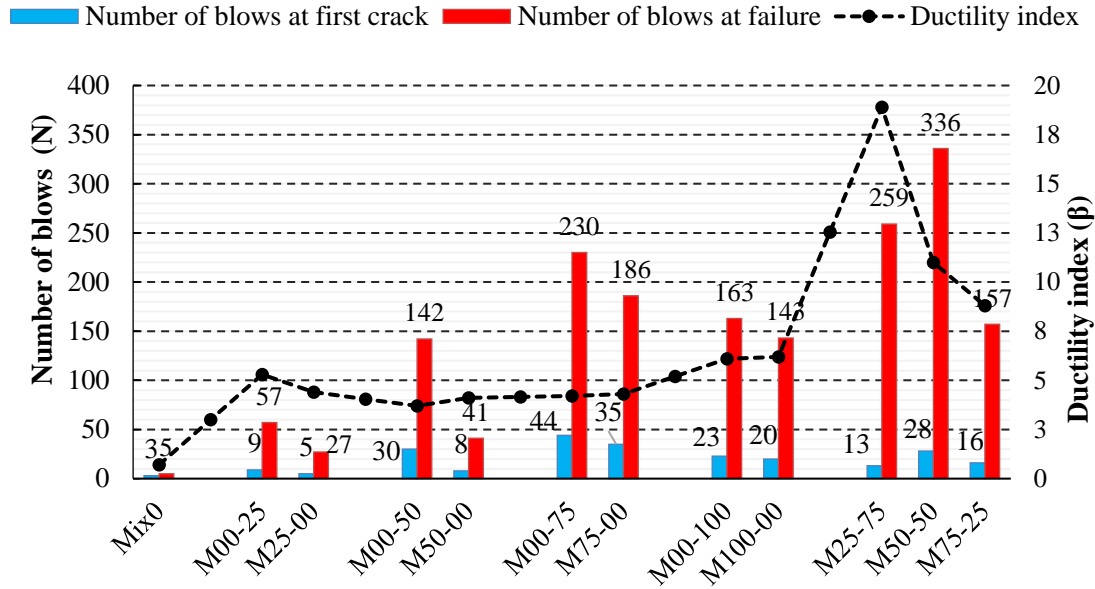


Fig. 11 Number of blows at first crack, Number of blows at failure and ductility index of HSC mixes with different volume fractions of MSP and MPF

1724.3, 4295.5, 6957.5 and 4930.8 J, respectively. As can be seen, in mixes with one type of fibers and the same volume fraction ratio, the impact energy at the first crack and failure for specimen with macro-polyolefin fibers was higher than specimen with micro-steel fibers. In hybrid mixes, the impact energy at the first crack even in the best case (M50-50) was lower than mixes with

0.75% macro polyolefin fibers and mixes with 0.75% and 0.5% micro steel fibers. However, hybrid mixes had a good performance in the impact energy at failure, so that M50-50 and M25-75 had the highest impact energy at failure among all the mixes. In terms of ductility index, micro steel fibers showed better performance than the mixes containing polyolefin fibers, except in volume ratio of 0.25%. However, in high volume ratio, such as 0.1%, this difference in ductility index was insignificant. The ability of fibers to enhance the impact resistance of concrete is primarily due to the significant amount of energy absorbed during the processes of fiber debonding, stretching, and being pulled out from the concrete matrix as cracks form and propagate. When cracking initiates in the concrete, the evenly dispersed fibers become engaged and act to restrict further crack growth and propagation. As a result, the strength and ductility of the fiber-reinforced concrete are both increased (Feng *et al.* 2018).

The fracture patterns of the specimens in the laboratory show that control specimens had significantly lower impact resistance than those reinforced with MSF and MPF. The failure of the control specimens occurred abruptly immediately after the creation of the initial crack, leading to the appearance of a diagonal cracking pattern. This type of brittle failure with a diagonal crack is the most commonly observed failure mode for plain concrete, which aligns with previous studies (Nili and Afroughsabet 2011, Ding *et al.* 2017, Mastali *et al.* 2017).

On the other hand, specimens containing MSF and MPF displayed a different behavior where

the impact resistance was meaningfully improved due to fiber presence. Due to the ability to withstand a greater number of impact blows, a circular fractured region developed centrally under the area struck by the steel ball. As the quantity of blows increased, the size of this fractured zone expanded. The MSF specimens predominantly failed by breaking into three pieces, while the MPF specimens failed either into three pieces (for M00-25 and M00-50 mixes) or four pieces (for M00-75 and M00-100 mixes). This different behavior between specimens with MSF and MPF arises from the fact that higher impact loads (a greater number of blows) are necessary to initiate the first crack and failure in the MPF specimens.

4. Conclusions

This study concentrates on investigating the influences of micro-steel fibers (MSF) and macro-polyolefin fibers (MPF) on the flexural performance and impact resistance of high-strength concrete (HSC). Based on the findings obtained from the current research, the following conclusions can be derived:

- The addition of both MSF and MPF fibers reduced the workability of fresh concrete. The effects of MSF and MPF on compressive strength were insignificant. The highest compressive strength was for hybrid mixes with 0.5% MSF and 0.5% MPF, which increased by 16.5% compared to the control sample.
- The area under the load-deflection curve, representing the energy absorption capacity, was significantly larger for the hybrid mixes and mixes containing only MSF when compared to those reinforced solely with MPF.
- The incorporation of MPF alone did not enhance the peak load capacity of HSC. However, a significant improvement in peak load was observed in hybrid mixes combining MPF with MSF and in mixes containing only MSF compared to the control sample.
- The flexural strength and toughness of HSC are substantially influenced by the type and volume fraction of fibers incorporated. Mixes containing MSF, particularly at higher volume fractions (above 0.25%), exhibited superior flexural strength and toughness compared to the control mix and mixes containing only MPF. The flexural toughness increased by up to 6.65 times for 1.0% MSF, while the maximum improvement for 1.0% MPF was only 3.41 times compared to the control sample.
- The volume fraction of fibers incorporated significantly governed the load-deflection behavior and post-peak load-carrying capacity of HSC. Higher fiber dosages, particularly in the case of MSF, led to improved load-bearing ability and enhanced performance after reaching the maximum load. This emphasizes the crucial role of fiber quantity in tailoring the post-cracking response and ductility of HSC, enabling better energy dissipation and crack resistance.
- The highest equivalent flexural strength ratios ($R_{T,150}^D$) were achieved in hybrid mixes combining MSF and MPF, reaching up to 79.1% for the M25-75 mix, indicating the synergistic benefits of fiber hybridization on flexural performance.
- The impact resistance based on the RBDWI test method demonstrated the significant enhancement of incorporating fibers. MSF and MPF substantially improved the impact energy at the first crack and failure compared to the control mix. While MPF mixes exhibited higher impact resistance at the first crack for a given fiber volume fraction, the hybrid fiber mixes displayed the best overall impact resistance at failure, notably the M50-50 and M25-75 mixes.

References

- Abna, A. and Mazloom, M. (2022), "Flexural properties of fiber reinforced concrete containing silica fume and nano-silica", *Mater. Lett.*, **316**, 132003. <https://doi.org/10.1016/j.matlet.2022.132003>.
- Ahmadi, S.H., Mazloom, M. and Salehi, H. (2024a), "Comparison of SEM and TPM methods for evaluating the effect of nano-silica and silica fume on the fracture behavior of SCLC", *J. Struct. Integr. Maint.*, **9**(3), 2392988. <https://doi.org/10.1080/24705314.2024.2392988>.
- Ahmadi, S.H., Mazloom, M. and Salehi, H. (2024b), "Total and initial fracture energies of self-compacting lightweight concrete containing silica fume and nano-silica", *Eng. Fract. Mech.*, **308**, 110382. <https://doi.org/10.1016/j.engfracmech.2024.110382>.
- ACI 544.3R-08 (2008), Guide for Specifying, Proportioning, and Production of Fiber-Reinforced Concrete, American Concrete Institute.
- ACI 544.9R-17 (2017), Report on Measuring Mechanical Properties of Hardened Fiber Reinforced Concrete, American Concrete Institute.
- Alberti, M.G., Enfedaque, A., Gálvez, J.C. and Álvarez, C. (2019), "Using polyolefin fibers with moderate-strength concrete matrix to improve ductility", *J. Mater. Civ. Eng.*, **31**(9), 04019170. [https://doi.org/10.1061/\(ASCE\)MT.1943-5533.0002775](https://doi.org/10.1061/(ASCE)MT.1943-5533.0002775).
- Alberti, M.G., Enfedaque, A., Gálvez, J.C. and Picazo, A. (2020), "Recent advances in structural fibre-reinforced concrete focused on polyolefin-based macro-synthetic fibres", *Constr. Build. Mater.*, **70**(337), e206-e206. <https://doi.org/10.3989/mc.2020.12418>.
- Altalabani, D., Bzeni, D.K. and Linsel, S. (2020), "Mechanical properties and load deflection relationship of polypropylene fiber reinforced self-compacting lightweight concrete", *Constr. Build. Mater.*, **252**, 119084. <https://doi.org/10.1016/j.conbuildmat.2020.119084>.
- Antarvedi, B., Banjara, N.K. and Singh, S. (2023), "Optimisation of polypropylene and steel fibres for the enhancement of mechanical properties of fibre-reinforced concrete", *Asian J. Civ. Eng.*, **24**(4), 1055-1075. <https://doi.org/10.1007/s42107-022-00553-6>.
- ASTM C143 (2020), Standard test method for slump of hydraulic-cement concrete, American Society of Testing and Materials.
- ASTM C1609/C1609M-12 (2012), Standard Test Method for Flexural Performance of Fiber-Reinforced Concrete (Using Beam With Third-Point Loading), ASTM International, West Conshohocken, PA.
- ASTM, C 138 (2014), Standard test method for density (unit weight), yield, and air content (gravimetric) of concrete. ASTM International West Conshohocken, PA, USA.
- BS 1881 (1983), Testing concrete-Part 116: method for determination of compressive strength of concrete cubes.
- Breitenbuecher, R. (1999), High performance fiber concrete SIFCON for repairing environmental structures. in Proceedings of the third RILEM/ACI workshop: high-performance fiber reinforced cement composites, London, UK.
- Cuenca, E., Echegaray-Oviedo, J. and Serna, P. (2015), "Influence of concrete matrix and type of fiber on the shear behavior of self-compacting fiber reinforced concrete beams", *Compos. Part B Eng.*, **75**, 135-147. <https://doi.org/10.1016/j.compositesb.2015.01.037>.
- Conforti, A., Tiberti, G., Plizzari, G.A., Caratelli, A. and Meda, A. (2017), "Precast tunnel segments reinforced by macro-synthetic fibers", *Tunn. Undergr. Sp. Tech.*, **63**, 1-11. <https://doi.org/10.1016/j.tust.2016.12.005>.
- Ding, Y., Li, D., Zhang, Y. and Azevedo, C. (2017), "Experimental investigation on the composite effect of steel rebars and macro fibers on the impact behavior of high performance self-compacting concrete", *Constr. Build. Mater.*, **136**, 495-505. <https://doi.org/10.1016/j.conbuildmat.2017.01.073>.
- Doostmohamadi, A., Karamloo, M. and Afzali-Naniz, O. (2020), "Effect of polyolefin macro fibers and handmade GFRP anchorage system on improving the bonding behavior of GFRP bars embedded in self-compacting lightweight concrete", *Constr. Build. Mater.*, **253**, 119230. <https://doi.org/10.1016/j.conbuildmat.2020.119230>.
- Fallah, S. and Nematzadeh, M. (2017), "Mechanical properties and durability of high-strength concrete

- containing macro-polymeric and polypropylene fibers with nano-silica and silica fume”, *Constr. Build. Mater.*, **132**, 170-187. <https://doi.org/10.1016/j.conbuildmat.2016.11.100>.
- Farnam, Y., Mohammadi, S. and Shekarchi, M. (2010), “Experimental and numerical investigations of low velocity impact behavior of high-performance fiber-reinforced cement-based composite”, *Int. J. Impact Eng.*, **37**(2), 220-229. <https://doi.org/10.1016/j.ijimpeng.2009.08.006>.
- Feng, J., Sun, W., Zhai, H., Wang, L., Dong, H. and Wu, Q. (2018), “Experimental study on hybrid effect evaluation of fiber reinforced concrete subjected to drop weight impacts”, *Mater.*, **11**(12), 2563. <https://doi.org/10.3390%2Fma11122563>.
- Ganesan, N. and Shivananda, K.P. (2000), “Strength and ductility of latex modified steel fibre reinforced concrete flexural members”, *J. Struct. Eng. (Madras)*, **27**(2) 111-116.
- Guo, H., Tao, J., Chen, Y., Li, D., Jia, B. and Zhai, Y. (2019), “Effect of steel and polypropylene fibers on the quasi-static and dynamic splitting tensile properties of high-strength concrete”, *Constr. Build. Mater.*, **224**, 504-514. <https://doi.org/10.1016/j.conbuildmat.2019.07.096>.
- Hadeed, M., Humad, A.M. and Al-Gburi, M. (2023), “Utilization of hybrid fibers in different types of concrete and their activity”, *J. Mech. Behav. Mater.*, **32**(1), 20220262. <https://doi.org/10.1515/jmbm-2022-0262>.
- Hakeem, I.Y., Amin, M., Abdelsalam, B.A., Tayeh, B.A., Althoey, F. and Agwa, I.S. (2022), “Effects of nano-silica and micro-steel fiber on the engineering properties of ultra-high-performance concrete”, *Struct. Eng. Mech.*, **82**(3), 295-312. <https://doi.org/10.12989/sem.2022.82.3.295>.
- Karamloo, M., Afzali-Naniz, O. and Doostmohamadi, A. (2020), “Impact of using different amounts of polyolefin macro fibers on fracture behavior, size effect, and mechanical properties of self-compacting lightweight concrete”, *Constr. Build. Mater.*, **250**, 118856. <https://doi.org/10.1016/j.conbuildmat.2020.118856>.
- Karimpour, A., Ghalehnovi, M., Edalati, M. and De Brito, J. (2021), “Properties of fibre-reinforced high-strength concrete with nano-silica and silica fume”, *Appl. Sci.*, **11**(20), 9696. <https://doi.org/10.3390/app11209696>.
- Karimpour, H. and Mazloom, M. (2022), “Pseudo-strain hardening and mechanical properties of green cementitious composites containing polypropylene fibers”, *Struct. Eng. Mech.*, **81**(5), 575-589. <https://doi.org/10.12989/sem.2022.81.5.575>.
- Karimpour, H. and Mazloom, M. (2023), “Multiple effects of nano-silica on the pseudo-strain-hardening behavior of fiber-reinforced cementitious composites”, *Adv. Nano Res.*, **15**(5), 467-484. <https://doi.org/10.12989/anr.2023.15.5.467>.
- Mastali, M., Dalvand, A. and Sattarifard, A. (2017), “The impact resistance and mechanical properties of the reinforced self-compacting concrete incorporating recycled CFRP fiber with different lengths and dosages”, *Compos. Part B Eng.*, **112**, 74-92. <https://doi.org/10.1016/j.compositesb.2016.12.029>.
- Mazloom, M. (2023), *Construction of Earthquake-Resistant Concrete and Steel Structures*, 1st Ed., Woodhead Publishing, Elsevier. <https://doi.org/10.1016/c2022-0-02687-8>.
- Mazloom, M., Abna, A., Karimpour, H. and Akbari-Jamkaraniand, M. (2023), “The crack propagation of fiber-reinforced self-compacting concrete containing micro-silica and nano-silica”, *Adv. Nano Res.*, **15**(6), 495-511. <https://doi.org/10.12989/anr.2023.15.6.495>.
- Mazloom, M., Afzali-Naniz, O. and Baratizadeh, H. (2023), “The fracture energy and mechanical properties of high-strength concrete containing polyolefin macro-fibres”, *Eur. J. Environ. Civil Eng.*, **27**(13), 3834-3848. <https://doi.org/10.1080/19648189.2022.2162135>.
- Mazloom, M. and Charmsazi M.E. (2024), “Investigating the combination of natural and crushed gravel on the fresh and hardened properties of self-compacting concrete”, *Struct. Monit. Maint.*, **11**(1), 1-18. <https://doi.org/10.12989/smm.2024.11.1.001>.
- Mazloom, M., Farahani Tajar, S. and Mahboubi, F. (2020), “Long-term quality control of self-compacting semi-lightweight concrete using short-term compressive strength and combinatorial artificial neural networks”, *Comput. Concrete*, **25**(5), 401-409. <https://doi.org/10.12989/cac.2020.25.5.401>.
- Mazloom, M., Mehrvand, M., Pourhaji, P. and Savaripour, A. (2019), “Studying the effects of CFRP and GFRP sheets on the strengthening of self-compacting RC girder”, *Struct. Monit. Maint.*, **6**(1), 47-66.

- <https://doi.org/10.12989/smm.2019.6.1.047>.
- Mazloom, M. and Mirzamohammadi, S. (2021), "Computing the fracture energy of fiber reinforced cementitious composites using response surface methodology", *Adv. Comput. Des.*, **6**(3), 225-239. <https://doi.org/10.12989/acd.2021.6.3.225>.
- Mazloom, M., Pourhaji, P. and Afzali Naniz, O. (2021), "Effects of halloysite nanotube, nano-silica and micro-silica on rheology, hardened properties and fracture energy of SCLC", *Struct. Eng. Mech.*, **80**(1), 91-101. <https://doi.org/10.12989/sem.2021.80.1.091>.
- Mazloom, M., Saffari, A. and Mehrvand, M. (2015), "Compressive, shear and torsional strength of beams made of self-compacting concrete", *Comput. Concrete*, **15**(6), 935-950. <https://doi.org/10.12989/cac.2015.15.6.935>.
- Mazloom, M., Salehi, H. and Akbari-Jamkarani, M. (2024), "Monitoring the effects of silica fume, copper slag and nano-silica on the mechanical properties of polypropylene fiber-reinforced cementitious composites", *Struct. Monit. Maint.*, **11**(2), 71-86. <https://doi.org/10.12989/smm.2024.11.2.071>.
- Mirzamohammadi, S. and Mazloom, M. (2021), "Monitoring the required energy for the crack propagation of fiber-reinforced cementitious composite", *Struct. Monit. Maint.*, **8**(3), 279-294. <https://doi.org/10.12989/smm.2021.8.3.279>.
- Navas, F.O., Navarro-Gregori, J., Herdocia, G.L., Serna, P. and Cuenca, E. (2018), "An experimental study on the shear behaviour of reinforced concrete beams with macro-synthetic fibres", *Constr. Build. Mater.*, **169**, 888-899. <https://doi.org/10.1016/j.conbuildmat.2018.02.023>.
- Nikzad, Y., Mazloom, M. and Parhizkari, M.H. (2024) "Effect of sand fineness modulus on SCC and SCLC properties", *Constr. Build. Mater.*, **421**, 135761. <https://doi.org/10.1016/j.conbuildmat.2024.135761>.
- Nili, M. and Afrouhsabet, V. (2010), "The effects of silica fume and polypropylene fibers on the impact resistance and mechanical properties of concrete", *Constr. Build. Mater.*, **24**(6), 927-933. <https://doi.org/10.1016/j.conbuildmat.2009.11.025>.
- Shen, D., Liu, X., Li, Q., Sun, L. and Wang, W. (2019), "Early-age behavior and cracking resistance of high-strength concrete reinforced with Dramix 3D steel fiber", *Constr. Build. Mater.*, **196**, 307-316. <https://doi.org/10.1016/j.conbuildmat.2018.10.125>.
- Shen, D., Wen, C., Zhu, P., Wu, Y. and Yuan, J. (2020), "Influence of Barchip fiber on early-age autogenous shrinkage of high strength concrete", *Constr. Build. Mater.*, **256**, 119223. <https://doi.org/10.1016/j.conbuildmat.2020.119223>.
- Shi, F., Pham, T.M., Hao, H. and Hao, Y. (2020), "Post-cracking behaviour of basalt and macro polypropylene hybrid fibre reinforced concrete with different compressive strengths", *Constr. Build. Mater.*, **262**, 120108. <https://doi.org/10.1016/j.conbuildmat.2020.120108>.
- Sorelli, L.G., Meda, A. and Plizzari, G.A. (2006), "Steel fiber concrete slabs on ground: a structural matter", *ACI Mater. J.*, **103**(4), 551.
- Song, P.S. and Hwang, S. (2004), "Mechanical properties of high-strength steel fiber-reinforced concrete", *Constr. Build. Mater.*, **18**(9) 669-673. <https://doi.org/10.1016/j.conbuildmat.2004.04.027>.
- Xue, J., Briseghella, B., Huang, F., Nuti, C., Tabatabai, H. and Chen, B. (2020), "Review of ultra-high-performance concrete and its application in bridge engineering", *Constr. Build. Mater.*, **260**, 19844. <https://doi.org/10.1016/j.conbuildmat.2020.119844>.